Journal of Alzheimer's Disease 43 (2015) 491–509
DOI 10.3233/JAD-141221
IOS Press

PKCε Deficits in Alzheimer's Disease Brains and Skin Fibroblasts

Tapan K. Khan*, Abhik Sen, Jarin Hongpaisan, Chol S. Lim, Thomas J. Nelson and Daniel L. Alkon
Blanchette Rockefeller Neurosciences Institute, Morgantown, WV, USA

Accepted 16 June 2014

Abstract. In Alzheimer's disease (AD) transgenic mice, activation of synaptogenic protein kinase C ε (PKCε) was found to prevent synaptotoxic amyloid-β (Aβ)-oligomer elevation, PKCε deficits, early synaptic loss, cognitive deficits, and amyloid plaque formation. In humans, to study the role of PKCε in the pathophysiology of AD and to evaluate its possible use as an early AD-biomarker, we examined PKCε and Aβ in the brains of autopsy-confirmed AD patients ($n = 20$) and age-matched controls (AC, $n = 19$), and in skin fibroblast samples from AD ($n = 14$), non-AD dementia patients ($n = 14$), and AC ($n = 22$). Intraneuronal Aβ levels were measured immunohistochemically (using an Aβ-specific antibody) in hippocampal pyramidal cells of human autopsy brains. PKCε was significantly lower in the hippocampus and temporal pole areas of AD brains, whereas Aβ levels were significantly higher. The ratio of PKCε to Aβ in individual CA1 pyramidal cells was markedly lower in the autopsy AD brains versus controls. PKCε was inversely correlated with Aβ levels in controls, whereas in AD patients, PKCε showed no significant correlation with Aβ. In autopsy brains, PKCε decreased as the Braak score increased. Skin fibroblast samples from AD patients also demonstrated a deficit in PKCε compared to controls and an AD-specific change in the Aβ-oligomer effects on PKCε. Together, these data demonstrate that the relationship between Aβ levels and PKCε is markedly altered in AD patients' brains and skin fibroblasts, reflecting a loss of protective effect of PKCε against toxic Aβ accumulation. These changes of PKCε levels in human skin fibroblasts may provide an accurate, non-invasive peripheral AD biomarker.

Keywords: Alzheimer's disease, amyloid-β oligomers, diagnostic assay, peripheral biomarker, PKCε

INTRODUCTION

Our understanding of the earliest events in the pathophysiologic progression of Alzheimer's disease (AD) remains limited, presenting a major obstacle to the development of new therapeutics that can prevent or slow neurodegeneration in AD, and the discovery of diagnostic biomarkers that can identify high-risk patients who may benefit from early treatment [1]. Studies of brains from postmortem AD patients and mouse models of AD have revealed that one of the earliest pathologic events is the loss of synapses in specific brain areas critical for memory, such as the hippocampus. This loss of synapses, and the associated cognitive deficits, has been shown to precede other pathologic hallmarks of AD, such as the deposition of amyloid plaques and neurofibrillary tangles [2–4]. Protein kinase C ε (PKCε) is predominantly expressed in the brain [5] and has recently been implicated in several aspects of AD pathophysiology [6, 7]. PKCε deficiency in the brain has been reported to occur early in AD progression in the Tg2576 transgenic mouse model [8]. Aβ has been shown to directly bind to a specific PKC pseudo-substrate domain (a 28–35 amino acid sequence) to block PKC activity [9]. Aging, the major risk factor for sporadic AD, is also associated with a deficit in PKCε [10]. Conversely, activation of PKCε has been shown to cause degradation of Aβ via the endothelin converting enzyme [7, 11], activation of α-secretase to generate the synaptogenic non-toxic soluble amyloid-β protein precursor α (sAβPPα) [12, 13], and reduction of GSK3-β activity [14], thereby decreasing hyperphosphorylation of tau. In neurons, activation of PKCε reduces Aβ oligomer-induced

*Correspondence to: Tapan K. Khan, Blanchette Rockefeller Neurosciences Institute, 8 Medical Center Drive, Morgantown, WV 26506, USA. Tel.: +1 304 293 0934; Fax: +1 304 293 3675; E-mail: tkhan@brni.org.

ISSN 1387-2877/15/$27.50

destruction of mature synapses and has been shown to enhance memory and prevent neuronal death [8, 15]. Other studies have shown that apolipoprotein E 3 (ApoE3) stimulates the synthesis of PKCε [16], thereby increasing synaptogenesis in cultured neuron networks.

In AD, therefore, loss of the synaptogenic and anti-apoptotic effects of PKCε, including PKCε-induced degradation of Aβ-oligomers, could be a crucial early event in AD that leads to synaptic loss and cognitive impairment and the eventual accumulation of Aβ and deposition of amyloid plaques and neurofibrillary tangles [8]. Therapies that maintain the balance between PKCε and Aβ-oligomers may protect synapses required to sustain cognitive functions such as learning and memory. Further, diagnostic assays that can detect an imbalance between PKCε and Aβ-oligomers may be able to identify patients at the earliest stages of the disease.

A growing body of evidence shows that AD is associated with changes in peripheral tissues, outside the central nervous system [17–25]. Amyloid pathogenesis and tau metabolic pathways are not limited to the brain, but are ubiquitous in the human body and found in blood, saliva, skin, and other peripheral tissues [20, 25, 26]. For example, primary human skin fibroblasts of symptomatic and presymptomatic patients carrying the Swedish familial AD mutation produce excess Aβ protein [17, 21]. AD-specific Aβ deposition has also been noted in the human lens [19], as well as AD-related abnormalities in blood cells [18, 22, 24] and Aβ deposition in blood vessels, skin, subcutaneous tissue, and intestine of AD patients [20]. Collectively, these findings suggest that AD pathophysiology has systematic expression while its phenotypic expression is brain-specific. Based on these observations, we hypothesized that PKCε in skin fibroblasts might serve as an accurate peripheral biomarker of AD that reflects changes in PKCε in the AD brain. In this study, we measured PKCε and Aβ levels in human autopsy brain samples and in fresh and banked skin fibroblast samples from patients with AD, patients with non-AD dementia (non-ADD), and age-matched controls to evaluate the diagnostic accuracy of skin fibroblast PKCε as a biomarker of AD.

MATERIALS AND METHODS

Human brain tissue samples

Freshly frozen and freshly fixed (for immunofluorescence microscopy) autopsy-confirmed AD ($n = 10$ hippocampus, $n = 10$ temporal pole area) and age-and gender-matched control (AC, $n = 9$ hippocampus, $n = 10$ temporal pole area) brain tissue slices were obtained from the Harvard Brain Tissue Resource Center, McLean Hospital, Boston, MA (Tables 1 and 2). Approval for the study was obtained from Dr. Francine M. Benes, Harvard Brain Tissue Resource Center, McLean Hospital. All patients (or their legal representatives) gave informed consent to provide brain tissue samples at autopsy, which was performed within 24 h of death. The pathological diagnosis of AD was conducted according to the Consortium to Establish a Registry for Alzheimer's Disease (CERAD). The study was carried out in accordance with the Code of Ethics of the World Medical Association (Declaration of Helsinki) for experiments involving humans (http://www.wma.net/en/30publications/10policies/b3/index.html).

Table 1
Patient ID and autopsy diagnosis of hippocampus area of Alzheimer's disease (AD) patients and age-matched control cases

Patient ID	Autopsy diagnosis	Age	Gender	Average age ± SD	% Female
AN15589	AD Braak 2	84	F	78.3 ± 10.5	50%
AN18056	AD Braak 4	88	F		
AN01667	AD Braak 5	68	M		
AN10254	AD Braak 6	78	M		
AN02930	AD Braak 3	80	M		
AN14554	AD Braak 6	61	F		
AN17726	AD Braak 2	72	M		
AN06468	AD Braak 4	98	M		
AN16195	AD Braak 5	73	F		
AN02773	AD Braak 5	81	F		
AN10329	Control	81	F	80.88 ± 8.77	50%
AN00704	Control	82	F		
AN00316	Control	75	F		
AN17896	Control	69	M		
AN12667	Control	86	M		
AN15515	Control	73	M		
AN08396	Control	76	M		
AN02921	Control	89	F		
AN03324	Control	97	M		

Human skin fibroblast samples

Skin fibroblast samples from 28 patients (AD: $n = 14$, 9 autopsy-confirmed AD; 3 genetically validated AD, and 2 clinically confirmed AD; non-AD dementia: $n = 14$, one autopsy-confirmed; 13 genetically validated), and 22 non-demented AC cases (n = 50) were obtained from the cell bank at the Coriell Institute for Medical Research (Camden, NJ; Tables 3). The number of cell lines used for each experiment is described in Table 3 (see footnotes). Fresh fibroblasts

Table 2
Patient ID, autopsy diagnosis and PKCε expression levels of temporal pole area of Alzheimer's disease (AD) patients versus age-matched control cases

Patient ID	Autopsy diagnosis	Age	Gender	PKCε (A.U.) (immunoblot)*	Average Age ± SD	% Female
AN02005	AD Braak 5	81	M	345.857	82.5 ± 6.3	50%
AN19148	AD Braak 5	82	F	471.888		
AN11070	AD Braak 5	86	F	433.533		
AN12095	AD Braak 6	90	F	480.835		
AN07090	AD Braak 6	80	M	311.959		
AN02485	AD Braak 5	73	M	391.273		
AN19950	AD Braak 5	84	M	370.288		
AN05080	AD Braak 4	90	F	360.301		
AN14738	AD Braak 5	87	M	402.133		
AN18776	AD Braak 6	72	F	273.495		
AN01877	Control	93	F	538.083	83 ± 6.9	50%
AN06400	Control	91	F	598.736		
AN06291	Control	87	M	561.813		
AN06291	Control	86	F	507.404		
AN02397	Control	85	M	419.806		
AN18592	Control	82	F	587.720		
AN06669	Control	81	M	608.417		
AN09667	Control	80	M	393.754		
AN09933	Control	73	M	237.759		
AN18904	Control	72	F	447.286		

*Average of at least three measurements. Student's *t*-test, type 1, one-tail distribution; $p < 0.01$.

were isolated from punch biopsy (2–3 mm, upper arm) skin samples taken from patients with clinically confirmed AD ($n = 5$) and AC ($n = 5$; Table 4). Biopsies were performed by qualified personnel under the supervision of Dr. Shirley Neitch and with the IRB approval of Marshall University (Huntington, WV). All patients (or their legal representatives) provided informed consent. The clinical diagnosis of AD was made by Dr. Neitch. The method of isolating and culturing fibroblasts from skin biopsies is described elsewhere [27, 28]. For this study, we used cells from passages 5 to 14.

Antibodies

Anti-amyloid-β peptide (MOAB-2) (Cat No: MABN254; Millipore, Billerica, MA) detects Aβ in soluble, oligomeric, and fibrillar forms in human AD brain tissue by immunofluorescence, according to the manufacturer. The antibody was specifically cloned (6C3) to recognize unaggregated, oligomeric, and fibrillar forms of $A\beta_{42}$ and $A\beta_{40}$, but not AβPP. An independent laboratory verified the application of this antibody to detect unaggregated forms of intraneuronal $A\beta_{42}$ and $A\beta_{40}$ but not intraneuronal AβPP by immunoblot and immunoprecipitation analysis in 5 × FAD mice brains [29]. The antibody for PKCε (C-15) (Santa Cruz Biotechnology, Santa Cruz, CA.; Cat No: sc-214) has been used to detect PKCε of human origin by immunoblotting and immunofluorescence analysis; a very recent study used the C-15 antibody for absolute quantitation of endogenous PKCε with high precision and accuracy using a capillary immunoelectrophoresis system [30]. Anti-β-tubulin, a class III rabbit monoclonal antibody (Millipore Corporation, Cat No: 04-1049), was used for normalization of protein loading in immunoblotting. Anti-β-actin antibody was obtained from Santa Cruz Biotechnology. Absolute concentration of PKCε was measured by ELISA using Human Protein Kinase C Epsilon (hPKCε) ELISA Kit (Antibodies-online.com). The manufacturer has recommended this sandwich enzyme immunoassay for the *in vitro* quantitative measurements of PKCε in human tissue homogenates.

Immunoblot analysis of cultured skin fibroblasts

Flasks containing cultured skin fibroblasts were washed three times with 1× PBS (pH 7.4), the cells were collected using a cell scraper, transferred to 1.5 ml microcentrifuge tubes, and centrifuged at 1000 rpm for 5 min. The cell pellet was suspended in homogenizing buffer (10 mM Tris pH 7.4, 1 mM PMSF, 10 mM EGTA, 10 mM EDTA, and 50 mM NaF) and sonicated for 30 s. The homogenate was centrifuged again at 4°C for 10 min at 10000 rpm and the supernatant was collected and transferred to a new tube. Total protein concentration was measured using a Bradford Protein assay Kit (Thermo Scientific, Rockford, IL). Protein samples (20 μg) were boiled in 2×

Table 3
In-depth demographics, genetic/family history, and clinical history of the banked patients[1]

	Cell ID	Age	Gender	Description
Alzheimer's disease (AD)				
1	AG08245*#^	75	M	Caucasian, No family history of AD. 7 y of disease duration before the biopsy, autopsy-confirmed AD. The skin biopsy was taken postmortem.
2	AG06263*#^	67	F	Caucasian, no family history of AD. This is a sporadic AD case by clinical diagnosis. 7 y of disease duration. The skin biopsy was taken antemortem.
3	AG14149*#	80	F	Caucasian, autopsy-confirmed AD with strong family history and APOE4 gene.
4	AG06840*#^	56	M	Canadian Caucasian, clinically confirmed familial AD with presenilin 1 (PSEN1) gene. History of progressive memory loss of one year. The skin biopsy was taken antemortem.
5	AG04401*#	53	F	Caucasian, autopsy-confirmed familial AD patient. The skin biopsy was taken ante-mortem.
6	AG06262*#	66	M	Caucasian, clinically confirmed AD with no family history. The skin biopsy was taken ante-mortem.
7	AG05770*#^	70	M	Caucasian, no family history of AD. 7.5 y of disease duration before the biopsy, autopsy-confirmed AD. The skin biopsy was taken postmortem.
8	AG04402*#	47	M	Caucasian, clinically affected member of a family with AD with signs of early dementia. Early-onset familial AD with APOE genotype.
9	AG10788*#^	87	Unknown	Caucasian, autopsy-confirmed AD with 17 y of disease duration. Family history of AD with ApoE4 gene. The biopsy was taken antemortem.
10	AG04159#^	52	F	Caucasian, clinically confirmed, familial Type 3 AD. The biopsy was taken antemortem.
11	AG05810#^	79	F	Jewish Caucasian, clinically affected with severe late stage dementia, typical of AD. Three siblings died with autopsy-confirmed AD. The biopsy was taken antemortem.
12	AG08527#^	61	M	German Caucasian, autopsy-confirmed AD. The biopsy was taken antemortem.
13	AG06844^	59	M	Caucasian, autopsy-confirmed familial type 3 AD; 11 y of disease duration. The biopsy was taken antemortem.
14	AG08259^	90	M	Caucasian, autopsy-confirmed AD with no family history; 3 y of disease duration. The biopsy was taken antemortem.
Non-Alzheimer's disease dementia (Non-ADD)				
1	GM04198*#^	63	F	Caucasian, clinically confirmed and genetically validated Huntington's disease.**
2	ND34265*#	62	M	Caucasian, clinically affected familial Parkinson's disease.
3	GM05030*#^	56	M	Caucasian, choreic movements with clinically confirmed and genetically validated Huntington's disease**.
4	GM06274*#^	56	F	Caucasian, clinically confirmed and genetically validated Huntington's disease.**
5	GM02165*#^	57	M	Caucasian, clinically confirmed and genetically validated Huntington's disease.**
6	GM02167*#	59	F	Caucasian, clinically confirmed and genetically validated Huntington's disease.**
7	ND31618*#	63	F	Caucasian, clinically affected familial Parkinson's disease.
8	AG08395*#	85	F	Caucasian, autopsy-confirmed Parkinson's disease. The skin biopsy was taken postmortem.
9	ND27760#^	55	F	Caucasian, familial Parkinson's disease Type 1; PARK1.**
10	GM20926#^	35	F	Lithuanian Caucasian, inclusion body myopathy with early-onset Paget disease and frontotemporal dementia**.
11	GM04226#^	74	M	Caucasian, clinically confirmed and genetically validated Huntington's disease.**
12	GM02173^	52	F	Caucasian, clinically confirmed and genetically validated Huntington's disease.**

Table 3
(*Continued*)

	Cell ID	Age	Gender	Description
13	GM00305^	56	F	Caucasian, clinically confirmed and genetically validated Huntington's disease.**
14	GM05031^	60	M	Caucasian, clinically confirmed and genetically validated Huntington's disease.**
Age-matched Control (AC)				
1	AG04058*#	53	M	Caucasian, non-demented age-matched control. The skin biopsy was taken antemortem.
2	AG07716*#	39	F	Caucasian, non-demented. The skin biopsy was taken antemortem.
3	AG06881*#	63	M	Caucasian, non-demented. The skin biopsy was taken antemortem.
4	AG07803*#	66	M	Caucasian, non-demented age-matched control. The skin biopsy was taken antemortem.
5	AG09555*	53	F	Caucasian, non-demented. The skin biopsy was taken antemortem.
6	AG09697*#	63	F	Caucasian, non-demented age-matched control. The skin biopsy was taken antemortem.
7	AG09977*#^	63	F	Caucasian, non-demented. The skin biopsy was taken antemortem.
8	AG09148*#	67	M	Caucasian, non-demented age-matched control. The skin biopsy was taken antemortem.
9	AG06242*#^	71	M	Caucasian, non-demented. The skin biopsy was taken antemortem.
10	AG04560*#^	59	M	Caucasian, non-demented. The skin biopsy was taken antemortem.
11	AG06237*#	45	M	Caucasian, non-demented. The skin biopsy was taken antemortem.
12	AG08044*	58	F	African American, non-demented. The skin biopsy was taken antemortem.
13	AG05840#	55	F	Caucasian, non-demented. The skin biopsy was taken antemortem.
14	AG07714#^	56	F	Caucasian, non-demented. The skin biopsy was taken antemortem.
15	AG11358#	71	M	Caucasian, non-demented. The skin biopsy was taken antemortem.
16	AG12998#^	65	M	Caucasian, non-demented. The skin biopsy was taken antemortem.
17	AG11734^	50	F	Caucasian, non-demented. The skin biopsy was taken antemortem.
18	AG05840^	55	F	Caucasian, non-demented. The skin biopsy was taken antemortem.
19	AG12927^	66	F	Caucasian, Non-demented. The skin biopsy was taken antemortem.
20	AG04461^	66	M	Caucasian, non-demented. The skin biopsy was taken antemortem.
21	AG11363^	74	F	Caucasian, non-demented. The skin biopsy was taken antemortem.
22	AG13358^	72	F	Caucasian, non-demented. The skin biopsy was taken antemortem.

[1]All information was obtained from the Coriell Cell Repository. *Cell lines used in PKCε ELISA-based slope/intercept assay (Fig. 7). #Cell lines used in PKCε ELISA-based basal level measurement (Fig. 6). ^Cell lines used in PKCε immunoblot-based basal level measurement (Fig. 4). **The time of biopsy taken was not reported as to whether it was antemortem or postmortem.

Laemmli buffer for 10 min and separated on 4–20% gradient Tris-Glycine gels. Separated proteins were transferred to nitrocellulose membrane and the membrane was blocked in BSA at room temperature (RT) for 15 min and incubated with 1 : 2000 dilution anti-PKCε rabbit polyclonal antibody and 1 : 5000 dilution anti-β-tubulin for 1 h at RT. The blot was washed three times with Tris-buffered saline-Tween 20 (TBS-T) and further incubated with alkaline phosphatase conjugated secondary antibody (Jackson Immunoresearch Laboratories, West Grove, PA) at 1 : 10,000 dilution for 45 min. The blot was washed three times

Table 4
In-depth demographics, genetic/family history, and clinical history of the samples from freshly taken biopsies*

Cell ID	Age	Gender	Description
Alzheimer's disease (AD) ($n = 5$)			
40M59-AD	59	M	Caucasian, clinically confirmed early-onset AD. After 7 y of disease duration, the punch biopsy was taken antemortem.
42M78-AD	78	M	Caucasian, clinically confirmed AD with no family history. This sporadic AD case had 2 y of disease duration at the time of punch biopsy. The skin biopsy was taken antemortem.
43M88-AD	88	M	Caucasian, clinically confirmed AD with no family history. This sporadic AD case had 9 y of disease duration at the time of punch biopsy. The skin biopsy was taken antemortem.
61M78-AD	78	M	Caucasian, clinically confirmed AD with no family history. This sporadic AD case had no record when the disease started. The skin biopsy was taken antemortem.
93F82-AD	82	F	Caucasian, clinically confirmed AD with no family history. This sporadic AD case had 9 y of disease duration at the time of punch biopsy. The skin biopsy was taken antemortem.
Age-matched Control (AC) (n = 5)			
80M45-AC	45	M	Caucasian, non-demented age-matched control. The skin biopsy was taken antemortem.
25M39-AC	39	M	Caucasian, non-demented control. The skin biopsy was taken antemortem.
39M65-AC	65	M	Caucasian, non-demented age-matched control. The skin biopsy was taken antemortem.
51M55-AC	55	M	Caucasian, non-demented age-matched control. The skin biopsy was taken antemortem.
78F45-AC	45	F	Caucasian, non-demented age-matched control. The skin biopsy was taken antemortem.

*All 10 samples (5 AD and 5 AC) were used in PKCε based ELISA.

with TBS-T and developed using the 1-step NBT-BCIP substrate (Thermo Scientific). Signal intensities of the images were recorded using ImageQuant RT-ECL (GE Life Sciences, Piscataway, NJ) and densitometric quantification was performed using IMAL software (Blanchette Rockefeller Neurosciences Institute, Morgantown, WV). Intensities of PKCε bands were normalized against β-tubulin for each lane.

Immunoblot analysis of temporal lobe tissue

Brain tissue was homogenized in 10 mM Tris-HCl (pH 7.4), 1 mM PMSF (phenylmethylsulfonyl fluoride), 1 mM EGTA, 1 mM EDTA, 50 mM NaF, and 20 μM leupeptin and lysed by sonication. Protein concentration was measured using the Coomassie Plus (Bradford) Protein Assay kit (Pierce, Rockford, IL). 20 μg of protein from each sample was subjected to SDS-PAGE analysis in 4–20% gradient Tris-Glycine gels (Invitrogen, Carlsbad, CA). All samples were loaded in the same gel. To avoid artifacts, the same order of sample loading was followed both for PKCε and β-actin blots. The separated protein was then transferred to nitrocellulose membrane. The membrane was blocked with 5% BSA at room temperature for 15 min and incubated with primary antibody (anti-PKCε and anti-β-actin) overnight at 4°C. After the incubation, the blot was washed three times with TBS-T and incubated with alkaline phosphatase conjugated secondary antibody at 1 : 10,000 dilution for 45 min. The membrane was washed three times with TBS-T and developed using the 1-step NBT-BCIP substrate. Blots were imaged in the ImageQuant RT-ECL and densitometric quantification was performed using the IMAL software.

Real-time quantitative RT-PCR

RNA was isolated from $\sim 1 \times 10^6$ cultured skin fibroblasts using Trizol reagent (Invitrogen) following the manufacturer's protocol. 2 μg of total RNA was reverse transcribed using oligodT and Superscript III (Invitrogen) at 50°C for 1 h. Two μl of the cDNA product was amplified using primers for PKCε (Forward: 5′-AGCCTCGTTCACGGTTCTATGC-3′, Reverse: 3′-GCAGTGACCTTCTGCATCCAGA-5′), and β-tubulin (Forward: 5′-TTGGGAGGTGATCAGCGATGAG-3′, Reverse: 3′-CTCCAGATCCACGAGCACGGC-5′) (Origene, Rockville, MD). Following a 25-cycle amplification at 55°C annealing temperature, the amplicons were analyzed in an E-Gel system (Invitrogen). The gel image was documented with a Fuji Image gel scanner (FLA-9000, Fuji Film, Hanover Park, IL) and densitometric quantification was performed using IMAL software (Blanchette Rockefeller Neurosciences Institute). Data were represented as

normalized ratios of PKCε optical density (OD) compared to β-tubulin OD for three independent experiments.

Preparation of amylospheroids (ASPDs)

ASPDs were prepared as published elsewhere [31, 32]. Briefly, $A\beta_{42}$ was dissolved in 1,1,1,3,3,3-hexafluoro-2-propanol (HFIP) and incubated overnight at 4°C followed by 3 h at 37°C. The dissolved $A\beta_{42}$ was lyophilized in 1.5-ml polypropylene centrifuge tubes at 40 nM/tube. The lyophilized Aβ was dissolved in PBS without Ca^{2+} or Mg^{2+} at <50 μM and centrifuged at 100 rpm for 14 h at 4°C. After incubation, the Aβ solution was purified using a 0.65-μm cutoff filter (Amicon Ultra, Millipore) to remove any fibrils. The final concentration of ASPDs was determined using a nanodrop spectrophotometer (Nanodrop 2000, Thermo Fisher, Pittsburgh, PA) ($\varepsilon 280 = 1490\ M^{-1}\ cm^{-1}$).

Measurement of PKCε in skin fibroblasts by ELISA

The absolute concentration of PKCε in skin fibroblast samples before and after treatment with ASPD (toxic amylospheroids derived from soluble oligomeric $A\beta_{42}$) was measured by ELISA using the hPKCε ELISA Kit (Antibodies-online.com), which has been recommended for the *in vitro* quantitative measurement of PKCε in human tissue homogenates. ELISA was performed on skin fibroblast samples from the following: 11 patients with non-AD dementia (non-ADD, 4 Parkinson's disease, 6 Huntington's disease (HD), and 1 frontotemporal disease), 17 patients with AD (5 autopsy-confirmed AD, 4 familial AD genes, and 8 clinically confirmed sporadic AD), and 20 AC, respectively (Table 3). Skin fibroblast cells were cultured to 100% confluency in low glucose DMEM medium supplemented with 10% serum. The medium was changed every three days. After treatment with ASPD (0, 50, 250, or 500 nM) for 16 h, the cells were washed three times with ice-cold 1 × PBS (~4 mL × 3 times/60 mm dish). A cold cocktail (100 μL) of 1× PBS containing protease and phosphatase inhibitors (pH 7.2) was added to each culture dish. The cells were collected by scraping and transferred into a new tube on ice followed by sonication. The supernatants were collected by centrifugation (10,000× g for 5 min) and stored at −80°C for ELISA assay. In some experiments, the proteasome was inhibited by co-administration of 5 μM lactacystin (Sigma Chemical, Cat#L6785) with toxic ASPD in each culture dish.

Measurement of intraneuronal PKCε and Aβ in hippocampal sections of autopsy-confirmed human brain by confocal microscopy

Intraneuronal PKCε and Aβ were measured by immunofluorescence microscopy in hippocampal sections from 10 autopsy-confirmed AD patients and 9 age-matched controls (Table 1). During autopsy, the hippocampi were removed and fixed at the Harvard site. Fixed hippocampi were dissected to 0.5–0.8 cm thickness and then immersed in fixative containing 10% formalin (postmortem interval range: 6.83–24 h). Hippocampi were sectioned into 0.4 cm slices with a vibratome (Leica VT1200S, Leica, Buffalo Grove, IL) and processed for paraffin embedding and sent to our site (Blanchette Rockefeller Neurosciences Institute, Morgantown, WV).

Paraffin-embedded sections were cut into 6-μm slices and deparaffinized with xylene, dehydrated with graded alcohol (100% to 50%), and washed with three times with 1 × PBS. Hippocampal slices were then treated with citrate buffer (10 mM citric acid at pH 6.0) added with 0.05% Tween 20 at 95°C for 30 min for antigen retrieval. After blocking non-specific protein binding with Image-iT^{TM} FX signal enhancer (Life Technologies, Grand Island, NY) for 1 h at RT, hippocampal sections were incubated with primary antibodies against PKCε (1 : 100, Santa Cruz Biotechnology), Aβ peptide (MOAB-2 antibody; 1 : 1000; Millipore), and neuron specific enolase (chicken polyclonal antibody; 1 : 75; Thermo Scientific, Rockford, IL) for 48 h at 4°C and then for 24 h at RT. Sections were then incubated with biotinylated horse anti-rabbit antibody (1 : 20; Vector Laboratories, Burlingame, CA) for 3 h at RT, and then with Alexa Fluor 568 goat anti-mouse IgG (1 : 200; Life Technologies), streptavidin conjugated with Alexa Fluor 488 (1 : 100; Life Technologies), and Alexa Fluor 647 goat anti-chicken IgG (1 : 100; Life Technologies) for 3 h at RT. Between each antibody incubation, all sections were washed 3 times for 5 min each time. Hippocampal sections were mounted on glass slides with Vectashield mounting medium with DAPI (Vector Laboratories) to counterstain nuclei and sealed with coverslips.

Hippocampal slices were oriented with a Zeiss Axio Observer Z1 microscope equipped with a 710 confocal scanning system using the 10× objective lens in the DAPI channel (for staining nuclei). The random CA1 area that appeared immediately after switching to the higher magnification lens, 63× Plan-APO Chromat oil immersion objectives (1.4 NA), was imaged for appropriate fluorescence used for quantification. Confocal

images of hippocampal sections were acquired in line scan mode and with a pinhole of approximately 1.00 Airy unit.

Statistical analyses

Statistical analyses were performed with Sigma Plot® 12.5 (Systat Software, Inc., San Jose, CA). The difference between two means was assessed by paired or unpaired *t*-test. The difference between multiple means was assessed by ANOVA. For all detail statistical analyses are presented in supplemental section. All pyramidal cells (127 for AC and 128 for AD cases) counted in confocal microscopy images of all hippocampus slices (9 AC and 10 AD patients autopsy brains) were included in the data analysis. Statistical data analysis of confocal images was followed as described elsewhere [8]. Briefly, all confocal images were first statistically analyzed by single factor ANOVA. Confocal data with a significant overall difference among the groups as demonstrated by ANOVA were further analyzed for between-group differences with paired two-tailed *t* test comparisons. Statistical analyses were followed as described elsewhere [33, 34]; a detailed description of all statistical analyses is provided in the supplemental materials.

RESULTS

Lower intraneuronal PKCε and higher Aβ-oligomer levels in CA1 pyramidal cells of hippocampi of autopsy AD brains

We used a PKCε-specific antibody and an Aβ-specific antibody for immunohistochemistry and confocal microscopy to quantify relative levels of PKCε and Aβ in CA1 pyramidal cells of hippocampi from AD and non-demented AC brain tissues, using the same method as previously published for 5 × FAD mouse brain tissues [29]. We examined a total of 128 pyramidal cells randomly selected from fresh-fixed brain slices from 10 autopsy-confirmed AD patients, and 127 pyramidal cells randomly selected from slices of 9 autopsy-confirmed AC cases (see patient population details in Table 1). To normalize for variations in fluorescence intensity between tissue samples, the fluorescence intensity of PKCε and Aβ were normalized to DAPI intensity within the same neuron. In CA1 neurons in AC brain slices, the intraneuronal PKCε levels were inversely correlated [polynomial, inverse first order: $f = y0 + (a/x)$; $p < 0.001$] with un-aggregated, oligomeric, and fibrillar Aβ levels (Fig. 1A, B). Non-linear fitting showed that the rate of decrease was faster at the lower Aβ concentration and this rate slowed after the PKCε-Aβ homeostasis was lost. In CA1 neurons of AD brain slices, there was no inverse relationship between intraneuronal PKCε and Aβ levels (Fig. 1A, C). In AD cases, the PKCε -Aβ correlation was lost ($p > 0.66$; non-significant), with a consistently lower level of PKCε compared with AC brains (see Supplemental Materials for detailed statistical analysis).

The intraneuronal PKCε level for each patient was calculated by averaging the levels from all CA1 cells per patient sample (Fig. 2A, B). For individual patients, the intraneuronal PKCε was inversely correlated with Aβ level for the AC cases ($n = 9$; slope $= -0.472 \pm 0.185$ (SEM); $p < 0.05$), whereas PKCε in AD cases showed no significant correlation with Aβ-oligomers ($n = 10$; slope $= -0{\cdot}0018 \pm 0{\cdot}071$ (SEM), $p > 1.00$; non-significant) (Fig. 2A, B). The level of PKCε in CA1 cells was significantly lower for AD versus AC cases ($p < 0.05$) (Fig. 2C). Conversely, the Aβ-oligomer level in CA1 pyramidal cells of human brains was significantly higher for AD patients versus AC cases ($p < 0.005$) (Fig. 2D). Therefore, the ratio of PKCε to Aβ-oligomers in individual patients was markedly lower in the AD brains compared to AC brains ($p < 0.03$) (Fig. 2E). Notably, Aβ-oligomer concentrations in hippocampal CA1 pyramidal cells increased with age in AC cases, but not in AD patients (Supplementary Fig. 1A, B).

Lower PKCε levels in the temporal poles of autopsy AD brains

To further study PKCε levels in another area of the brain known to be affected by AD pathology, we examined the levels of PKCε by immunoblot analysis in the temporal pole area of autopsy brain samples from AD patients ($n = 10$) and AC ($n = 10$) (see patient population details in Table 2). We found that the PKCε levels in the temporal poles of human brains were significantly lower for AD cases versus AC ($p < 0.025$; Fig. 3A, B). Using linear regression analysis, the PKCε levels in the temporal poles of AD and AC brains were inversely proportional to the Braak score, a measure of the amount of fibrillary tangles produced by hyperphosphorylation of tau (Fig. 3C; see Supplemental Materials for detailed statistical analysis). This is the first direct measure of PKCε levels in relation to phosphorylated tau (Braak score) in autopsy AD brains.

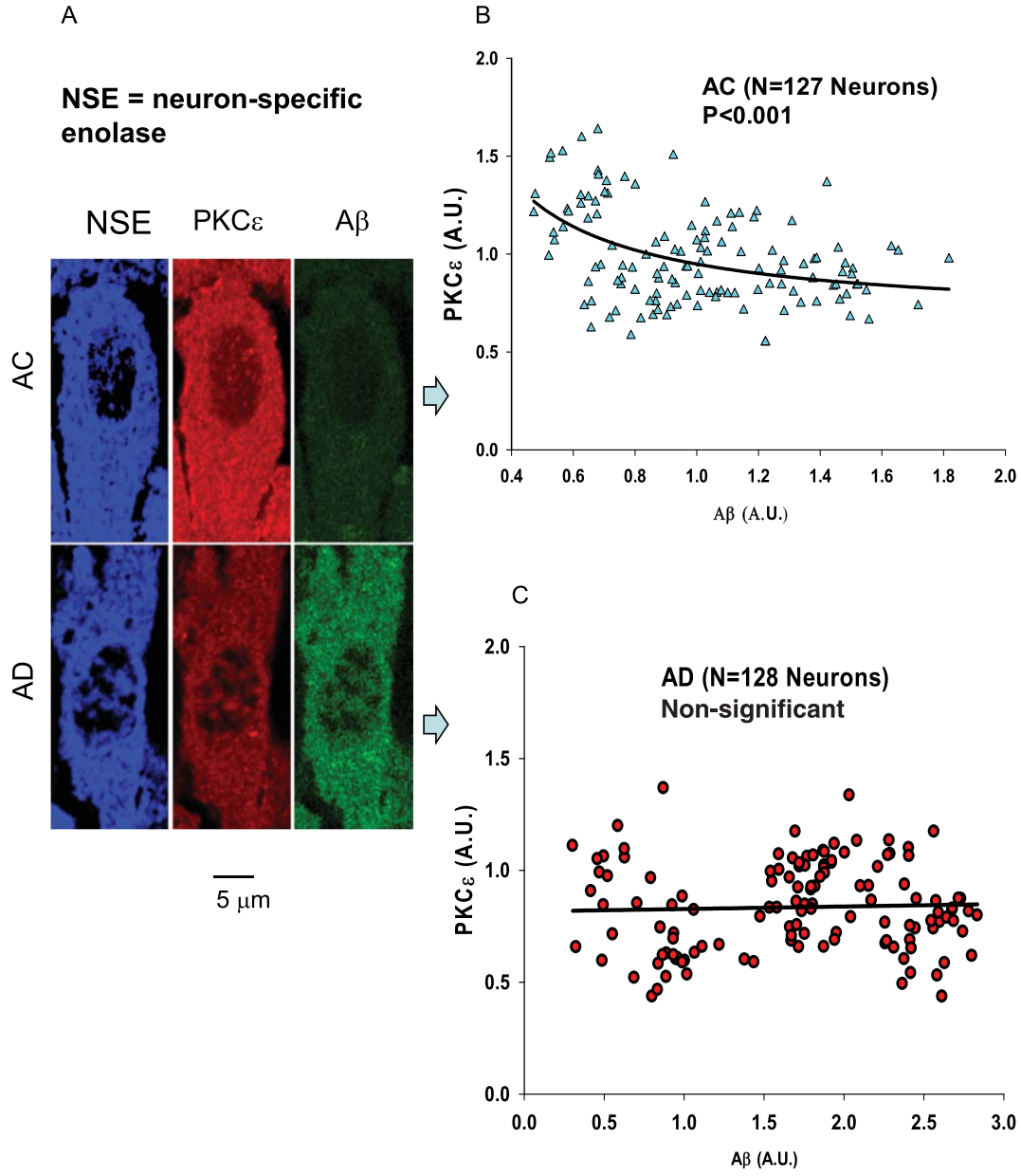

Fig. 1. Intraneuronal PKCε and Aβ levels in CA1 pyramidal cells of human autopsy brains measured by immunohistochemistry and confocal microscopy. A) Immunohistochemistry of neuron-specific enolase (NSE; a marker for neuronal cells), PKCε, and amyloid oligomers in CA1 pyramidal cells of human hippocampus, imaged by a confocal microscopy using PKCε- and Aβ-specific antibodies. To normalize for variations in fluorescence intensity between tissue samples, the fluorescence intensity of PKCε and Aβ were normalized to DAPI intensity within the same neuron. In CA1 pyramidal cells of age-matched control (AC) human hippocampus, the PKCε level was inversely correlated [polynomial, inverse first order: $f = y0 + (a/x)$] with Aβ (un-aggregated, oligomeric, and fibrillar) level (B); this relationship was not seen in the AD patient group (C). Each data point corresponds to a single CA1 pyramidal cell; 127 pyramidal cells were randomly selected from the slices of all 10 autopsy-confirmed AD patients, and 128 pyramidal cells were randomly selected from the slices of all 9 autopsy-confirmed AC cases. Data, shown in the figure and used for statistical analysis, were fluorescence ratios of PKCε and DAPI (PKCε /DAPI), and Aβ and DAPI (Aβ/DAPI) within the same neuron to normalize variable factors between tissue samples, included that human brain autopsies were not prepared at the same time.

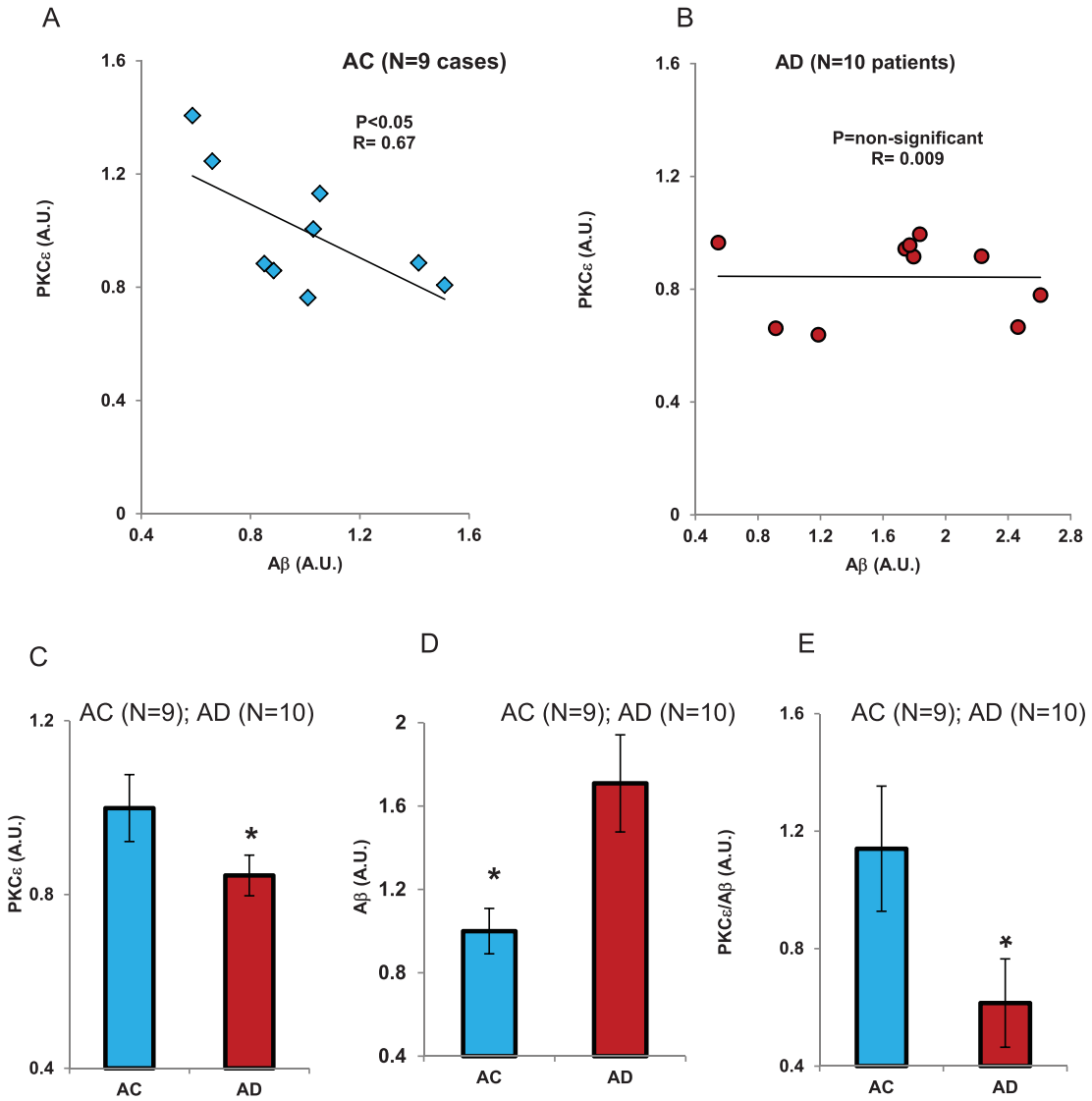

Fig. 2. Intraneuronal PKCε and Aβ levels in CA1 pyramidal cells of individual patient's autopsy brain. The PKCε and Aβ levels were averaged from all measured neurons for each patient. To normalize or variations in fluorescence intensity between tissue samples, the fluorescence intensity of PKCε and Aβ were normalized by DAPI intensity within the same neuron. The PKCε levels were inversely correlated with Aβ levels for age-matched control (AC, $n=9$) group (A); this relationship was not seen in the AD ($n=10$) patient group (B). C) When compared to the AC group, PKCε levels were lower in AD patients (t-test; $p<0.05$). D) The concentration of Aβ-oligomers in CA1 cells was higher in AD patients compared to AC cases (t-test; $p<0.005$). E) The average ratio of PKCε to Aβ for individual CA1 cells (PKCε /Aβ) was significantly higher for AC cases compared to AD patients (t-test; $p<0.02$). Data, shown in the figure and used for statistical analysis, were fluorescence ratios of PKCε and DAPI (PKCε /DAPI), and Aβ and DAPI (Aβ/DAPI) within the same neuron to normalize variable factors between tissue samples, included because the autopsies were not performed at the same time.

Lower levels of PKCε in cultured skin fibroblasts from AD patients

We obtained skin fibroblast samples from a tissue bank (Coriell Cell Repository, Camden, NJ; Tables 3), as well as from fresh tissue sources through our clinical collaborators at Marshall University (Table 4). Banked skin fibroblast samples ($n=10$) included 6 cases of sporadic AD (late onset, without family history), and 4 cases of familial (early-onset) AD; 9 out of the 10 AD samples were autopsy-confirmed. We performed an immunoblot analysis of PKCε in the 10 banked AD skin fibroblast samples, in addition to banked cell samples from 11 AC and 10 non-AD

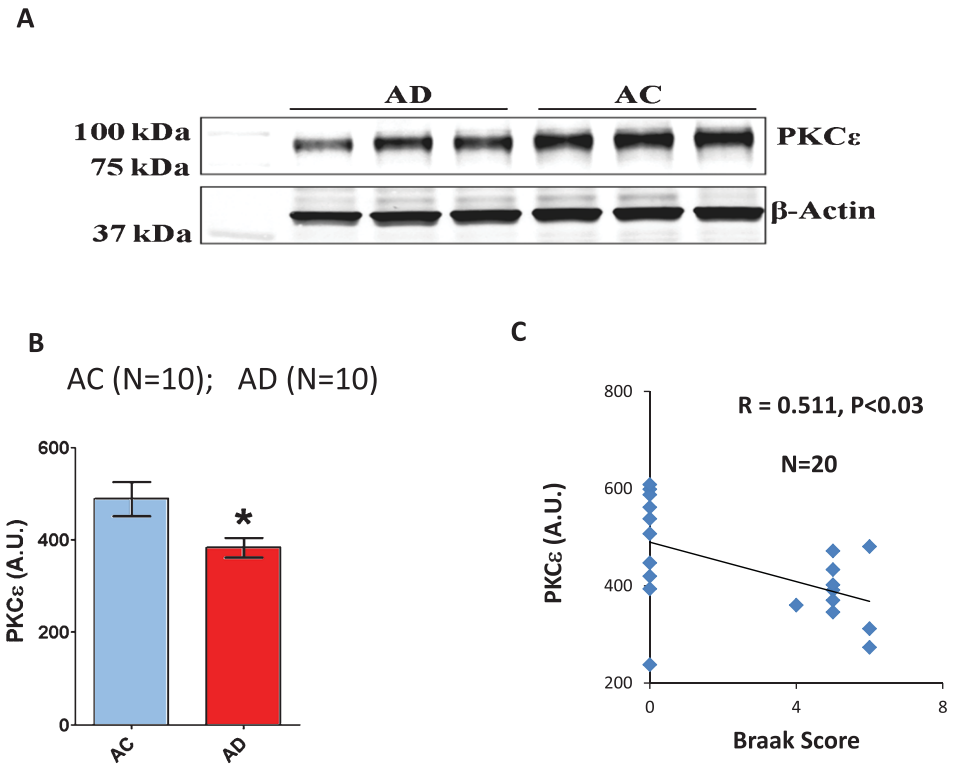

Fig. 3. PKCε levels in temporal lobe and Braak score in autopsy-confirmed Alzheimer's disease (AD) brains. A, B) The PKCε levels in the temporal lobe of human brains was significantly lower for AD cases ($n = 10$) to age-matched controls (AC, $n = 10$) measured by immunoblot with β-actin as loading control ($p < 0.025$). C) PKCε levels in the temporal lobe of human brains from AD patients and AC cases ($n = 20$) was inversely correlated with the Braak score.

dementia patients. PKCε levels in the AD skin fibroblasts were approximately 40% lower compared to AC samples ($p < 0.0001$; Fig. 4). In AC cells, the ratios varied between 0.7–1.2; in the non-AD dementia cells, the ratios varied between 0.72–1.3 (with one exceptions, HD6); and in AD cells, the ratios of all the cell lines were below 0.6. Mean values across each set of skin fibroblast samples were 0.857 ± 0.0361 (SEM) in AC cells, 1.040 ± 0.288 in non-AD dementia cells, and 0.501 ± 0.021 in AD cells. PKCε was significantly lower in AD compared to AC ($p < 0.0001$) and non-AD dementia ($p < 0.04$) skin fibroblast samples. The mean value for AC11 (0.621 ± 0.040) was the lowest among the ACs; however, it was also statistically significantly different when compared separately with all AD cases ($p < 0.02$). Values are reported as means ± SEM for at least three independent experiments.

The average normalized ratio of PKCε to β-tubulin was 0.857 ± 0.036 (SEM) in AC, 1.040 ± 0.288 in non-AD dementia, and 0.501 ± 0.021 in AD skin fibroblast samples. While one AC sample had a low mean basal PKCε level (Fig. 4B, AC11, 0.6213 ± 0.040), it was statistically significantly higher than the PKCε level in all AD cases ($p < 0.017$).

The data from the immunoblot analyses of PKCε in banked skin fibroblast samples were confirmed in immunofluorescence analyses (Supplementary Fig. 2). The average intensities of FITC-tagged PKCε in AC and AD cells were 18.092 ± 2.087 and 9.110 ± 1.420, respectively, $p < 0.05$. We also examined PKCε expression at the transcript level in the banked skin fibroblast samples. The average mRNA levels of PKCε compared to β-tubulin were determined by RT-PCR for 3 AD, 3 AC, and 2 HD banked skin fibroblast samples (Fig. 5A). The normalized average PKCε mRNA level for the AD skin fibroblast samples was significantly lower than that of the AC and HD samples (*t*-test, $p < 0.003$; AC: 0.904 ± 0.103, AD: 0.530 ± 0.061, and HD: 0.701 ± 0.143; Fig. 5B).

To measure the levels of PKCε in skin fibroblasts in a more quantitative manner, we used a high-throughput PKCε ELISA kit. We examined PKCε levels in both banked and fresh skin fibroblast samples and verified that the levels of PKCε were lower in AD skin fibrob-

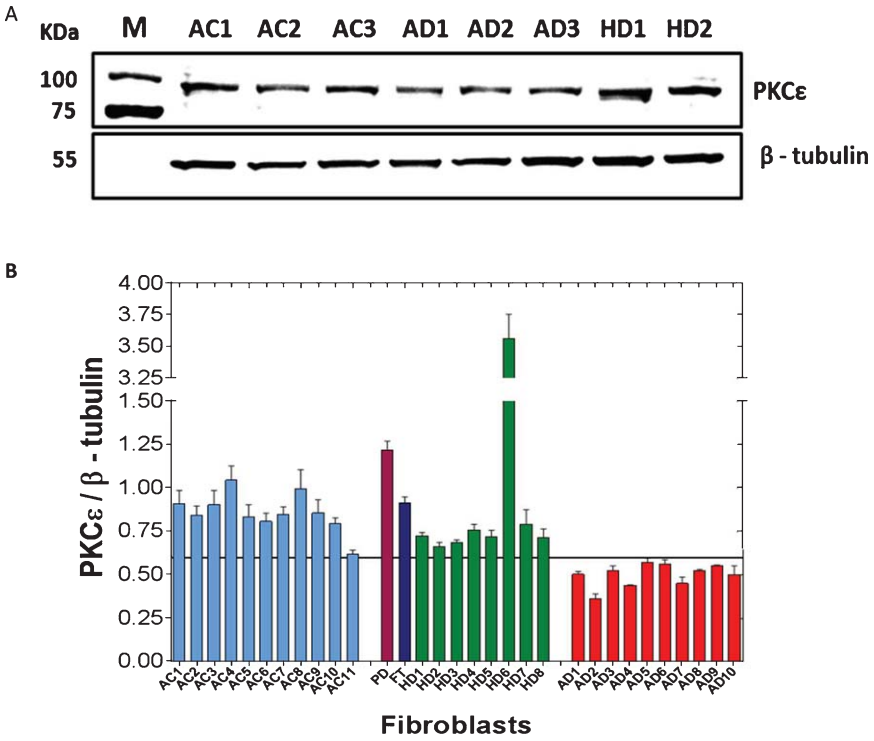

Fig. 4. PKCε expression in banked cultured human fibroblasts from age-matched controls (AC), Alzheimer's disease (AD), and non-AD dementia. A) Immunoblot of PKCε and β-tubulin in AC, AD, and non-AD dementia banked and cultured fibroblasts. AC1, AC2, and AC3 (AG07714, AG11734, and AG12927) are skin fibroblasts from age-matched controls; AD1, AD2, and AD3 (AG06844, AG04159, and AG08245) are from autopsy-confirmed AD patients; and HD1 and HD2 (GM06274, GM04198) are from Huntington's disease patients. B) Graphical representation of normalized densitometric ratios of PKCε to β-tubulin in skin fibroblast samples from 11 AC cases, 10 autopsy-confirmed AD patients, 8 HD patients, 1 Parkinson's disease (PD) patient, and 1 patient with frontotemporal dementia (FT). In AC cells, the ratios varied between 0.7–1.2; in the non-AD dementia cells, the ratios varied between 0.72–1.3 (with one exceptions, HD6); and in AD cells, the ratios of all the cell lines were below 0.6. [Cell lines: AD1 = AG06844, AD2 = AG04159, AD3 = AG06840, AD4 = AG08245, AD5 = AG05770, AD6 = AG08527, AD7 = AG06263, AD8 = AG10788, AD9 = AG08259, AD10 = AG05810; AC1 = AG07714, AC2 = AG11734, AC3 = AG05840, AC4 = AG12927, AC5 = AG06242, AC6 = AG04461, AC7 = AG11363, AC8 = AG09977, AC9 = AG12998, AC10 = AG04560, AC11 = AG13358; PD = ND27760, FT = GM20926, HD1 = GM06274, HD2 = GM02173, HD3 = GM00305, HD4 = GM04198; HD5 = GM05031, HD6 = GM02165, HD7 = GM04226, HD8 = GM05030].

lasts compared to non-ADD cases and AC (Fig. 6A, AD versus AC $p < 0.0002$; AD versus non-AD dementia $p < 0.0004$).

Toxic oligomeric Aβ reduced PKCε levels in cultured skin fibroblasts

We next examined the relationship between PKCε levels in skin fibroblasts and the presence of Aβ-oligomers. The most toxic soluble Aβ-oligomers are those prepared from $Aβ_{42}$ as ASPDs [31, 32]. We previously reported a toxic effect of ASPDs on PKCε that was greater than that of ADDL (Aβ-derived diffusible ligands) containing 12-mers, whereas Aβ-monomers caused no reduction in PKCε [15, 31, 32]. Treatment of cultured skin fibroblasts from AC ($n = 20$) with 500 nM ASPDs caused a decrease in PKCε to the levels seen in AD skin fibroblasts (Fig. 6A, C). A similar reduction in PKCε levels was seen in skin fibroblasts from non-ADD ($n = 11$) patients (data not shown), but not in fibroblasts from AD cases ($n = 17$) after treatment with ASPDs (500 nM derived from soluble oligomeric $Aβ_{42}$) (Fig. 6B). ASPD treatment led to an increase in PKCε in skin fibroblasts from AD patients (Fig. 6B). The effect of ASPD treatment on PKCε was similar for both banked and freshly isolated skin fibroblasts.

Similar to the relationship between PKCε and Aβ observed in the hippocampal CA1 pyramidal neurons in AC brain slices, PKCε levels in AC skin fibroblasts were inversely correlated with increasing concentrations of externally added Aβ-oligomers (ASPD) (slope = -0.0007 ± 0.0001 [SEM] ng/mL/μg

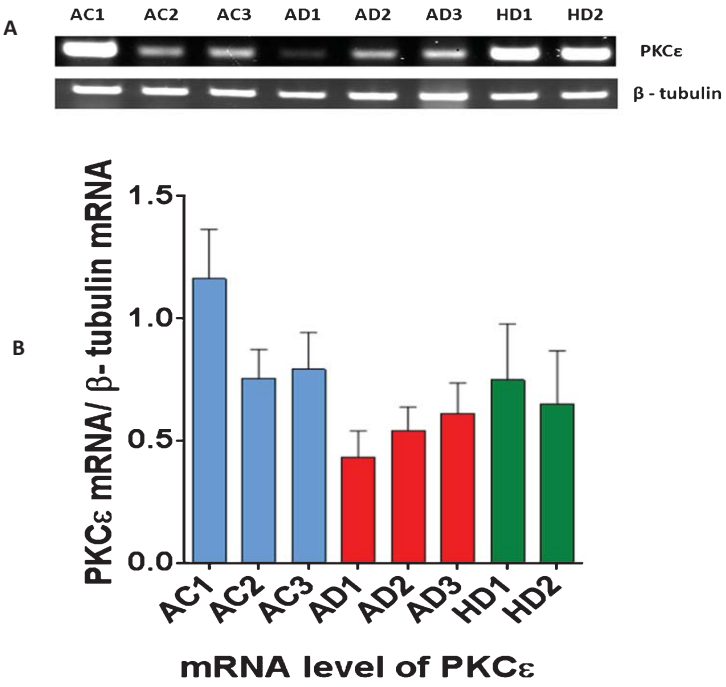

Fig. 5. RT-PCR analysis of PKCε in cultured skin fibroblasts. A) mRNA was isolated from the banked skin fibroblast samples from 3 AC, 3 AD, and 2 HD patients (AC1, AC2, and AC3: AG11363, AG09977, and AG12998, respectively; AD1, AD2, and AD3: AG06263, AG10788, and AG08259, respectively; HD1 and HD2: GM02165 and GM04226, respectively; Table 3). RT-PCR amplicons of PKCε and β-tubulin were run on E-Gels and imaged on a Fuji gel scanner. B) Histogram representing the amount of PKCε transcript normalized to β-tubulin for the 8 skin fibroblast samples. Values represent mean ± SEM for least three independent experiments.

PKCε protein/nM Aβ) (Fig. 6D). In contrast, the lower basal PKCε levels in AD skin fibroblasts showed a positive correlation with Aβ-oligomers (slope = 0.0005 ± 0.0001 [SEM] ng/mL/μg PKCε protein/nM Aβ) (Fig. 6E).

Differential effect of Aβ-oligomer (ASPD) treatment on PKCε in cultured skin fibroblasts: A potential diagnostic biomarker for AD

To further quantify the observed changes in PCKε levels in response to ASPD in AD versus AC skin fibroblasts, we calculated the slopes ($\times 10^{-4}$ ng/mL/μg PCKε protein/nM Aβ) and intercepts (ng/mL/μg PCKε protein) of PKCε levels in individual skin fibroblast samples treated with increasing concentrations of ASPD. The absolute quantities of PKCε were measured by ELISA (Fig. 7A). Almost all AC skin fibroblast samples ($n = 17$) showed negative slopes, whereas all AD skin fibroblast samples ($n = 14$) produced positive slopes. Plots of the intercepts versus slopes for each tested skin fibroblast sample distinguished AD skin fibroblasts (AD, red, within the box) from controls (AC, green) and other non-AD dementia (non-ADD, blue) patients from banked cells ($n = 29$) and cells isolated and cultured from freshly taken punch biopsies ($n = 10$). There was also no difference in PKCε levels between familial and sporadic AD groups and no difference in the slope of the PKCε versus ASPD linear plot between two groups.

Based on the intercept versus slope plots, two diagnostic criteria for an AD-positive skin fibroblast PKCε ELISA were defined: a slope >1.01 and an intercept <1.2. These two criteria showed high AD diagnostic accuracy, sensitivity, and specificity for detecting AD based on the response of skin fibroblasts to ASPD treatment (Fig. 7B, D). The slope/intercept was also found to be proportional to disease duration ($n = 9$) (Fig. 7C), which was calculated from the date of biopsy and the day the first symptoms of dementia were observed (see Supplemental Materials for detailed statistical analysis).

Proteasome blocking increases PKCε

Proteasome blocking by lactacystin increased the relative concentration of PKCε in AC tissues in the presence of ASPD. As a result, we found an increase

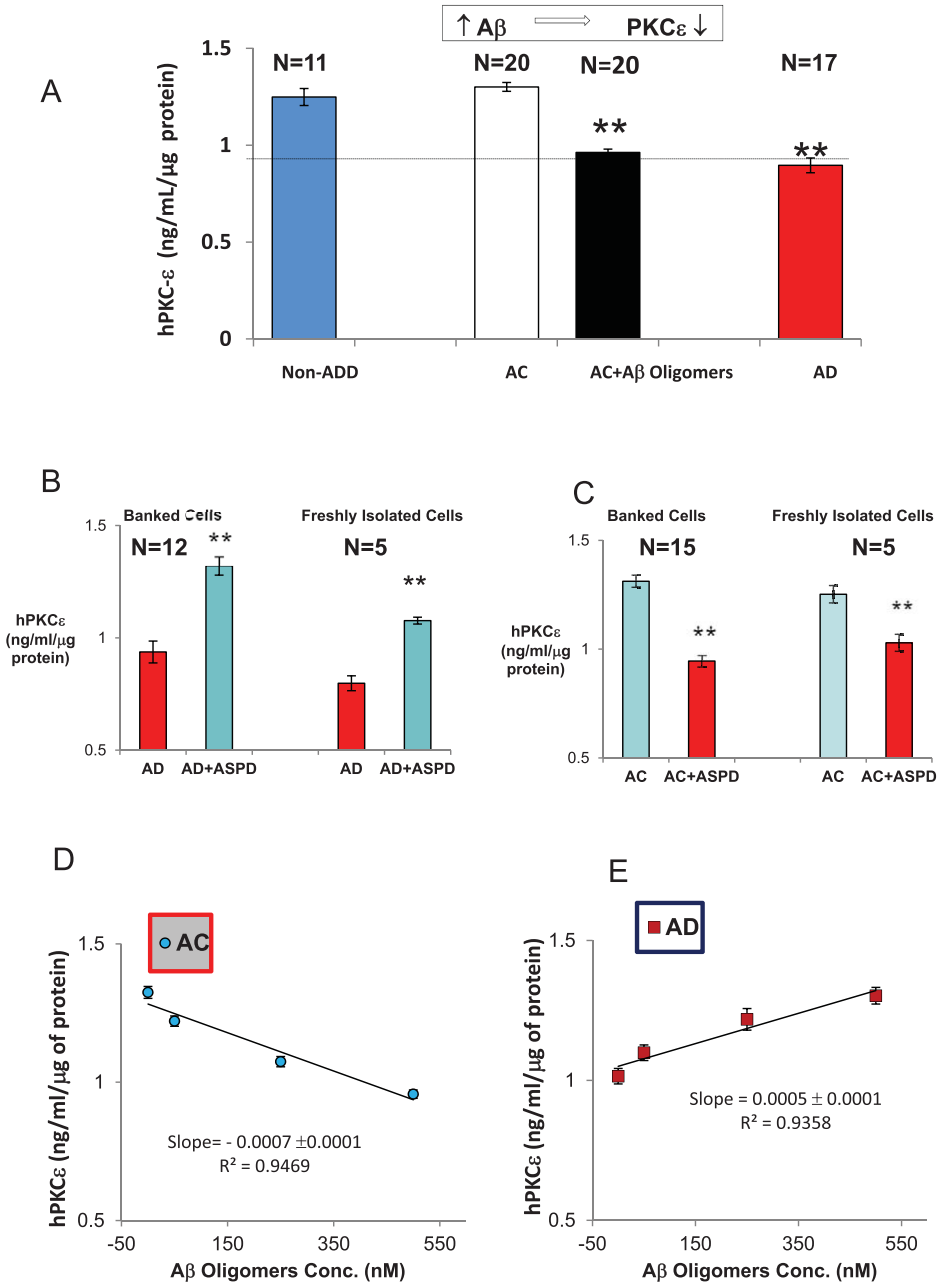

Fig. 6. Reduced levels of PKCε in cultured skin fibroblasts from Alzheimer's disease (AD) patients. The absolute quantity of PKCε (hPKCε, ng/mL/μg protein) levels in banked and fresh skin fibroblast samples was measured by ELISA specific to human PKCε. A) PKCε levels in human skin fibroblasts from non-AD dementia (non-ADD; $n = 11$, Table 3) and age-matched control (AC; $n = 20$, 15 from Table 3 and 5 from Table 4; AG08044 was not included) cases were higher than in AD patient samples ($n = 17$; 12 from Tables 3 and 5 from Table 4). B, C) Effect of soluble toxic oligomeric spheroidal amyloid (ASPD) treatment on the levels of PKCε in AD and AC skin fibroblasts (*t*-test statistical analysis: banked cell lines: $p < 0.00001$ for AC versus AC + ASPD and $p < 0.00005$ for AD versus AD + ASPD; freshly isolated cell lines: $p < 0.0004$ for AC versus AC + ASPD and $p < 0.00004$ for AD versus AD + ASPD). When treated with ASPD (500 nM toxic amylospheroids derived from soluble oligomeric $A\beta_{42}$), the levels of PKCε in AC skin fibroblasts was decreased to levels seen in AD skin fibroblasts. The basal level of PKCε was low in both banked ($n = 12$) and freshly isolated ($n = 5$) AD skin fibroblasts and increased after ASPD treatment. C) Basal levels of PKCε were high in both banked ($n = 17$) cells and freshly isolated ($n = 5$) AC skin fibroblasts and decreased after ASPD treatment. D) PKCε levels in cultured AC skin fibroblasts were inversely correlated with the concentration of externally added Aβ-oligomers (ASPD) (slope = -0.0007 ± 0.0001 [SEM], ng/mL/μg PKCε protein/nM Aβ). E) The lower basal PKCε levels in AD skin fibroblasts showed a positive correlation with increasing concentration of ASPD (slope = 0.0005 ± 0.0001 [SEM], ng/mL/μg PKCε protein/nM Aβ).

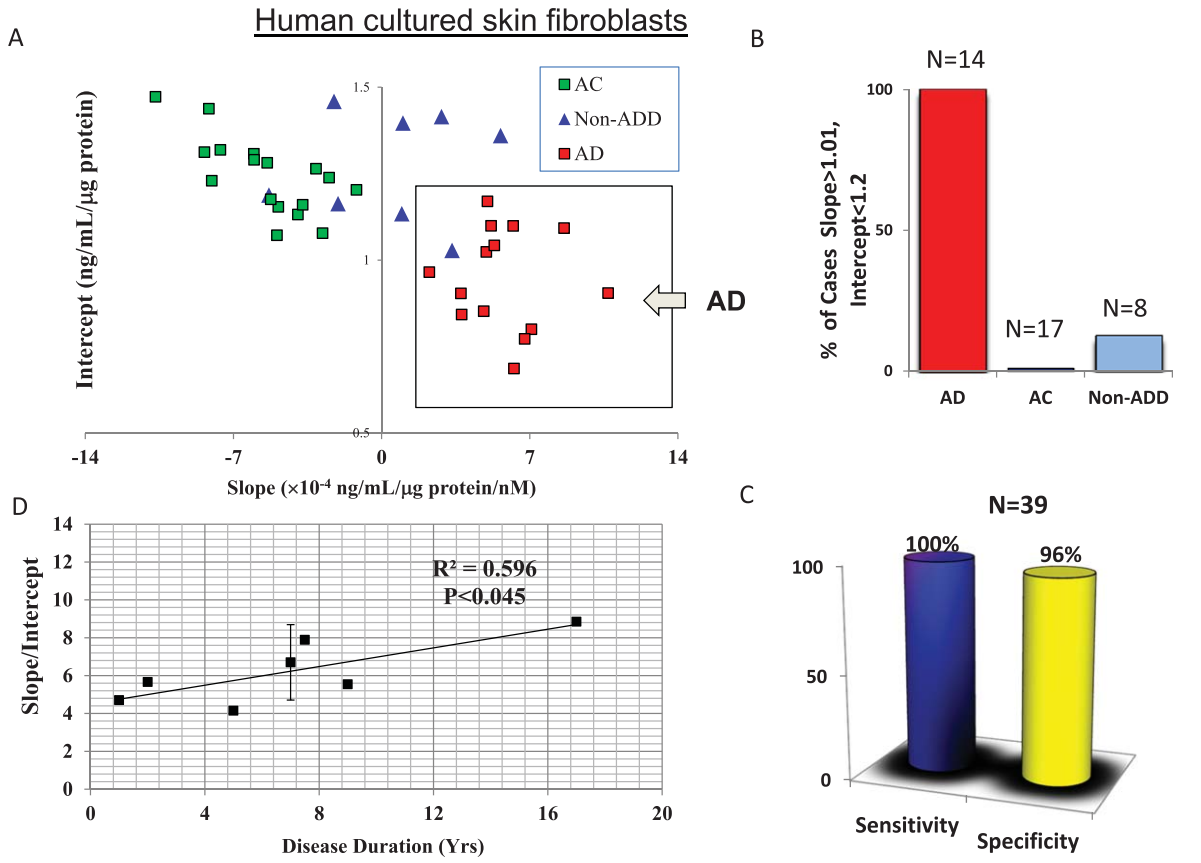

Fig. 7. Differential PKCε levels in response to toxic amylospheroids (ASPD): a potential peripheral biomarker of AD. A) Slopes and intercepts were calculated based on measuring absolute quantities of PKCε by ELISA after treatment of skin fibroblast samples with increasing concentrations of ASPD (0, 100, 250, and 500 nM). Intercept versus slope plots distinguished AD skin fibroblasts (AD, red) from AC (green) and non-ADD (blue) skin fibroblasts ($n = 39$ (29 banked and 10 fresh samples); AD = 14 (9 from Table 4 (banked) and 5 from Table 5 (freshly taken from clinic), AC = 17 (12 from Table 4 (banked) and 5 from Table 5 (freshly taken from clinic), Non-ADD = 8 (all banked). B) Diagnostic criteria and diagnostic performance of a skin fibroblast PKCε biomarker of AD. C) The sensitivity and specificity of the skin fibroblast PKCε biomarker of AD. D) The slope/intercept value was proportional to the disease duration ($n = 9$). We had indeed 9 points ($n = 9$ patients, in plots there are 7 points) in the plot. Three individual had the same disease duration. In fact the error bar was estimated from those three points.

in slope (from a high negative slope to a lower negative slope; Table 6, Fig. 8) in the PKCε versus ASPD plot for AC cases. This suggests that degradation of PKCε occurs via the proteasome pathway in AC tissues. In contrast, when we blocked the proteasome with lactacystin in AD cases, we found a decrease in slope (from a high positive slope to a lower positive slope; Table 6, Fig. 8) in the PKCε versus ASPD plots.

DISCUSSION

Using a variety of methods, we demonstrated that, in human brain tissues from autopsies and both banked and fresh skin fibroblast samples, the balance between Aβ-oligomers and PKCε levels in normal control tissues is markedly altered in AD. The results reported here in human tissues are consistent with previous findings in AD transgenic mice and provide compelling support for further validation of Aβ-induced changes in skin fibroblast PKCε as a new diagnostic marker for AD.

PKC isozymes, particularly α and ε, play a critical role in regulating major aspects of AD pathology including the loss of synapses, the generation of Aβ and amyloid plaques, and the GSK-3β-mediated hyperphosphorylation of tau in neurofibrillary tangles. Expression levels of different PKC isozymes in different brain regions and cultured skin fibroblasts have been summarized from previous studies (Table 5). To the best of our knowledge, this is the first report of PKCε levels in human brain tissue and cultured skin fibroblasts from patients with AD, non-ADD, and age-matched controls. We found that in both fresh

Table 5
PKC isozymes in AD brain and cultured skin fibroblasts

Isozyme	Brain					
	Brain region	M	C	Total	Method	Reference
PKCα	Hippocampus	↓	↑	NC	Immunoreactivity	[36]
	Frontal Cortex	NC	NC	NC	Immunoreactivity	[36]
	Temporal cortical tissue	↓	NC	ND	Immunoreactivity	[37]
PKCβI	Hippocampus	↓	↑	↑	Immunoreactivity	[36]
	Cortex	NC	↑	↑	Immunoreactivity	[36]
	Temporal cortical tissue	↓	NC	ND	Immunoreactivity	[37]
PKCβII	Hippocampus	↓	NC	↓	Immunoreactivity	[36]
	Frontal Cortex	↓	↑	↑	Immunoreactivity	[36]
PKCγ	Hippocampus	NC	NC	NC	Immunoreactivity	[36]
	Frontal Cortex	NC	NC	NC	Immunoreactivity	[36]
	Temporal cortical tissue	NC	↓	ND	Immunoreactivity	[37]
	Peripheral					
	Brain region	M	C	Total	Method	Reference
PKCα	Cultured fibroblasts	–	–	↓	Immunoreactivity	[38]
PKCγ	Cultured fibroblasts	–	–	NC	Immunoreactivity	[38]

M, Membrane; C, Cytosol; NC, No change; ND, Not determined.

Table 6
Change in slope of PKCε versus ASPD plots after blocking the proteasome with lactacystin in cultured human skin fibroblasts in the presence of ASPD

	Slope				Slope		
AC Cell Line	Without Lactacystin	With Lactacystin	% Change in slope	AD Cell Line	Without Lactacystin	With Lactacystin	% Change in slope
AG08044	−3.211	−0.933	70.94	AG10788	6.612	2.669	−59.63
0078F45*	−3.104	−2.244	27.71	0093F82*	2.258	2.585	14.48
AG04560	−6.548	−6.309	3.65	AG06262	8.608	3.885	−54.87
AG06242	−8.034	−4.581	42.99	AG05570	8.622	7.345	−14.81
AG09970	−12.036	−9.805	18.54				
Average percentage increase 32.77 ± 12.84 (SEM)				Average percentage decrease 28.71 ± 16.57 (SEM)			

*Fresh sample obtained from the clinic. AC, age-matched control; AD, Alzheimer's disease.

frozen autopsy brains and skin fibroblast samples, basal PKCε was lower in AD patients compared to age-matched controls. Furthermore, while there was a significant inverse correlation between PKCε and soluble Aβ oligomers in the brain and skin fibroblast samples from normal controls, this correlation was lost in the tissues from AD patients. In normal tissues, the inverse correlation between Aβ with PKCε is likely based on their reciprocal inhibitory effects, which maintains a homeostatic balance. In early AD, we hypothesize that a loss of this balance leads to a reduction in PKCε, a loss of PKCε-mediated inhibition of Aβ, and a subsequent increase in Aβ and the progression of the disease.

In our diagnostic assay, toxic Aβ oligomers added to AC fibroblasts reduced PKCε to levels observed for AD patients, but increased the lower basal levels of PKCε in fibroblasts from AD patients. We hypothesized that this effect reflects activation of proteasome degradation of PKCε in AC tissues that is lost in AD tissues. To test this hypothesis, the proteasome pathway blocker, lactacystin, was co-administered with toxic Aβ oligomers. As expected, in ACs, the proteasome blocker greatly reduced the Aβ-induced reduction of PKCε. Consequently, we found that in PKCε versus ASPD plots, the negative slope increased to a less negative slope for AC cases ($n = 5$) and the positive slope decreased to less positive slope for AD cases ($n = 4$, $p < 0.01$) (Fig. 8). In other words, lactacystin blocked PKCε degradation and increased the basal level of PKCε in both AC and AD cases, leading to a 'blunting' of the PKCε versus ASPD plot slopes. This indicates that proteasome-mediated degradation of PKCε is not lost in AD, and that the higher PKCε in AD cells (after ASPD treatment) rather represents *de novo* synthesis of PKCε. After the addition of ASPD to these AC cells, PKCε decreased, therefore we had a negative correlation and a negative slope. But in AD, there was an abnormal *de novo* synthesis of PKCε, perhaps in an effort by the cell to degrade the high Aβ levels and

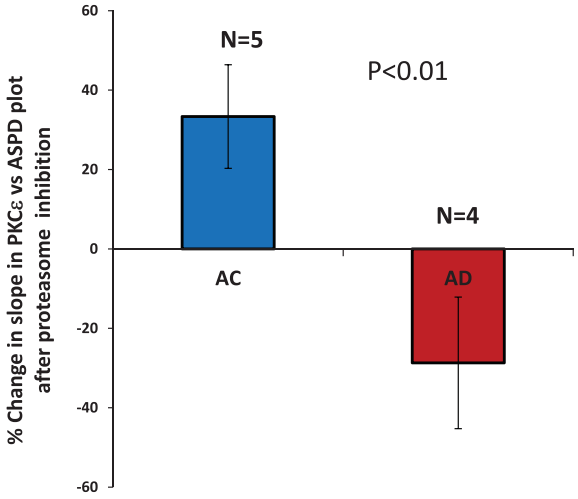

Fig. 8. Effect of proteasome inhibition on differential PKCε levels in response to toxic amylospheroids (ASPD) in cultured human skin fibroblasts from age-matched controls (AC) and Alzheimer's disease (AD) patients. Percent change in slope of PKCε versus ASPD plot. For AC cases, the slope increased to become less negative ($n = 5$); for AD cases, the slope decreased to become less positive ($n = 4$), $p < 0.01$.

bring the levels back to normal. Addition of ASPD to these cells just triggers more PKCε synthesis, leading to a positive slope. In AD cells, the normal homeostatic relationship between PKCε and Aβ is lost, with abnormal *de novo* synthesis of PKCε in AD but not AC that can be detected as a difference in slope by the assay. The abnormal mechanism of *de novo* synthesis of PKCε induced by ASPD is an area of active investigation in the lab.

Taken together, the results reported here for human brain and peripheral skin fibroblasts reinforce the clinical relevance of previous pre-clinical observations in mouse models of AD, and implicate PKCε loss as a marker of early AD. Our ELISA-based assay found that the loss of the inverse relationship between PKCε–Aβ oligomers in skin fibroblasts can accurately distinguish between tissues from AD patients and age-matched controls. This assay may detect an early pathologic event in AD—the imbalance of the reciprocal inhibition of PKCε and Aβ oligomers—that is recapitulated in the peripheral tissues and thus may provide an opportunity for development of new diagnostic assays for AD. Whereas in non-AD patients, PKCε regulates and reduces elevation of Aβ oligomers, the reverse could begin to predispose the patient to AD. Namely, if PKCε decreases in the aged brain (or with the ApoE4 mutation), Aβ oligomers rises and suppresses PKCε. Signs of an abnormal PKCε and Aβ balance, with *de novo* synthesis of PKCε in response to Aβ, could indicate that a patient is predisposed to AD. The low sample size is one of the limitations of the present study; we are currently validating PKCε as a biomarker of AD in a larger number of clinical samples collected from multiple sources.

Braak score, a well-proven quantitative representation of neurofibrillary tangles, is one of the gold standards of AD diagnosis at brain autopsy. In the present study, we found with increasing Braak score the PKCε levels decreased. To the best of our knowledge this is the first direct measure of PKCε levels in relation to phosphorylated tau (Braak score) in autopsy AD brains.

These results suggest, therefore, a potentially important relationship of reduced PKCε to AD pathology. The observations reported above document this PKCε-Aβ oligomer relationship in both brain tissues and peripheral (skin) tissues. Thus, these findings provide further support for the systemic expression of AD pathophysiology while symptomatic expression is restricted to the brain. Factors that have systemic impact, such as genetics, hypoxia, ischemia, and metabolic dysfunction could, therefore, be critically important in the etiology of AD.

ACKNOWLEDGMENTS

We thank Dr. Louis Fernandes and Dr. Francine M. Benes (Harvard Brain Tissue Resource Center, McLean Hospital, MA) for providing brain samples. We would also like to thank Dr. Camilla Forssten from Alere Inc. for her ongoing valuable discussions and Alere Diagnostics for their alliance support. Finally, we are also deeply grateful to Dr. Shirley Neitch from Marshall University, Huntington, WV, for her oversight and the clinical diagnosis for clinically obtained skin samples. We thank Ms. Dee DeNuto for helping in manuscript preparation and Dr. Florin Chirila for data analysis and helpful discussion. This research was supported in part by the Intramural Research Program of The Blanchette Rockefeller Neurosciences Institute, Morgantown, WV.

Authors' disclosures available online (http://www.j-alz.com/disclosures/view.php?id=2395).

SUPPLEMENTARY MATERIAL

The supplementary material is available in the electronic version of this article: http://dx.doi.org/10.3233/JAD-141221.

REFERENCES

[1] Mangialasche F, Solomon A, Winblad B, Mecocci P, Kivipelto M (2010) Alzheimer's disease: Clinical trials and drug development. *Lancet Neurol* **9**, 702-716.

[2] Coleman P, Federoff H, Kurlan R (2004) A focus on the synapse for neuroprotection in Alzheimer disease and other dementias. *Neurology* **63**, 1155-1162.

[3] Scheff SW, Price DA, Schmitt FA, Mufson EJ (2006) Hippocampal synaptic loss in early Alzheimer's disease and mild cognitive impairment. *Neurobiol Aging* **27**, 1372-1384.

[4] Terry RD, Masliah E, Salmon DP, Butters N, DeTeresa R, Hill R, Hansen LA, Katzman R (1991) Physical basis of cognitive alterations in Alzheimer's disease: Synaptic loss is the major correlate of cognitive impairment. *Ann Neurol* **30**, 572-580.

[5] Wetsel WC, Khan WA, Merchenthaler I, Rivera H, Halpern AE, Phung HM, Negro-Vilar A, Hannun YA (1992) Tissue and cellular distribution of the extended family of Protein Kinase C isoenzymes. *J Cell Biol* **117**, 121-133.

[6] Alkon DL, Sun MK, Nelson TJ (2007) PKC signaling deficits: A mechanistic hypothesis for the origins of Alzheimer's disease. *Trends Pharmacol Sci* **28**, 51-60.

[7] Nelson TJ, Cui C, Luo Y, Alkon DL (2009) Reduction of beta-amyloid levels by novel protein kinase C (epsilon) activators. *J Biol Chem* **284**, 34514-34521.

[8] Hongpaisan J, Sun MK, Alkon DL (2011) PKCε activation prevents synaptic loss, Aβ elevation, and cognitive deficits in Alzheimer's disease transgenic mice. *J Neurosci* **31**, 630-643.

[9] Lee W, Boo JH, Jung MW, Park SD, Kim YH, Kim SU, Mook-Jung I (2004) Amyloid-β peptide directly inhibits PKC activation. *Mol Cell Neurosci* **26**, 222-231.

[10] Hongpaisan J, Xu C, Sen A, Nelson TJ, Alkon DL (2013) PKC activation during training restores mushroom spine synapses and memory in the aged rat. *Neurobiol Dis* **55**, 44-62.

[11] Choi DS, Wang D, Yu GQ, Zhu G, Kharazia VN, Paredes JP, Chang WS, Deitchman JK, Mucke L, Messing RO (2006) PKCepsilon increases endothelin converting enzyme activity and reduces amyloid plaque pathology in transgenic mice. *Proc Natl Acad Sci U S A* **103**, 8215-8220.

[12] Lanni C, Mazzucchelli M, Porrello E, Govoni S, Racchi M (2004) Differential involvement of protein kinase C alpha and epsilon in the regulated secretion of soluble amyloid precursor protein. *Eur J Biochem* **271**, 3068-3075.

[13] Etcheberrigaray R, Tan M, Dewachter I, Kuipéri C, Van der Auwera I, Wera S, Qiao L, Bank B, Nelson TJ, Kozikowski AP, Van Leuven F, Alkon DL (2004) Therapeutic effects of PKC activators in Alzheimer's disease transgenic mice. *Proc Natl Acad Sci U S A* **101**, 11141-11146.

[14] Takashima A (2006) GSK-3 is essential in the pathogenesis of Alzheimer's disease. *J Alzheimers Dis* **9**(3 Suppl.), 309-317.

[15] Olds JL, Anderson ML, McPhie DL, Staten LD, Alkon DL (1989) Imaging of memory-specific changes in the distribution of protein kinase C in the hippocampus. *Science* **245**, 866-869.

[16] Sen A, Alkon DL, Nelson TJ (2012) Apolipoprotein E3 (ApoE3) but not ApoE4 protects against synaptic loss through increased expression of protein kinase C epsilon. *J Biol Chem* **287**, 15947-15958.

[17] Citron M, Vigo-Pelfrey C, Teplow DB, Miller C, Schenk D, Johnston J, Winblad B, Venizelos N, Lannfelt L, Selkoe DJ (1994) Excessive production of amyloid beta-protein by peripheral cells of symptomatic and presymptomatic patients carrying the Swedish familial Alzheimer disease mutation. *Proc Natl Acad Sci U S A* **91**, 11993-11997.

[18] Eckert A, Cotman CW, Zerfass R, Hennerici M, Müller WE (1998) Lymphocytes as cell model to study apoptosis in Alzheimer's disease: Vulnerability to programmed cell death appears to be altered. *J Neural Transm Suppl* **54**, 259-267.

[19] Goldstein LE, Muffat JA, Cherny RA, Moir RD, Ericsson MH, Huang X, Mavros C, Coccia JA, Faget KY, Fitch KA, Masters CL, Tanzi RE, Chylack LT Jr, Bush AI (2003) Cytosolic beta-amyloid deposition and supranuclear cataracts in lenses from people with Alzheimer's disease. *Lancet* **361**, 1258-1265.

[20] Joachim CL, Mori H, Selkoe DJ (1989) Amyloid beta-protein deposition in tissues other than brain in Alzheimer's disease. *Nature* **341**, 226-230.

[21] Johnston JA, Cowburn RF, Norgren S, Wiehager B, Venizelos N, Winblad B, Vigo-Pelfrey C, Schenk D, Lannfelt L, O'Neill C (1994) Increased beta-amyloid release and levels of amyloid precursor protein (APP) in fibroblast cell lines from family members with the Swedish Alzheimer's disease APP670/671 mutation. *FEBS Lett* **354**, 274-248.

[22] Perry RH, Wilson ID, Bober MJ, Atack J, Blessed G, Tomlinson BE, Perry EK (1982) Plasma and erythrocyte acetylcholinesterase in senile dementia of Alzheimer type. *Lancet* **1**, 174-175.

[23] Scheuner D1, Eckman C, Jensen M, Song X, Citron M, Suzuki N, Bird TD, Hardy J, Hutton M, Kukull W, Larson E, Levy-Lahad E, Viitanen M, Peskind E, Poorkaj P, Schellenberg G, Tanzi R, Wasco W, Lannfelt L, Selkoe D, Younkin S (1996) Secreted amyloid beta-protein similar to that in the senile plaques of Alzheimer's disease is increased *in vivo* by the presenilin 1 and 2 and APP mutations linked to familial Alzheimer's disease. *Nat Med* **2**, 864-870.

[24] Sevush S, Jy W, Horstman LL, Mao WW, Kolodny L, Ahn YS (1998) Platelet activation in Alzheimer disease. *Arch Neurol* **55**, 530-536.

[25] Heinonen O, Soininen H, Syrjänen S, Neittaanmäki H, Paljärvi L, Kosunen O, Syrjänen K, Riekkinen P Sr (1992) Amyloid beta-protein deposition in skin of patients with dementia, *Lancet* **339**, 245.

[26] Bermejo-Pareja F, Antequera D, Vargas T, Molina JA, Carro E (2010) Saliva levels of Aβ42 as potential biomarker of Alzheimer's disease: A pilot study. *BMC Neurol* **10**, 108.

[27] Khan TK, Alkon DL (2006) An internally controlled peripheral biomarker for Alzheimer's disease: Erk1 and Erk2 responses to the inflammatory signal bradykinin. *Proc Natl Acad Sci U S A* **103**, 13203-13207.

[28] Zhao WQ, Ravindranath L, Mohamed AS, Zohar O, Chen GH, Lyketsos CG, Etcheberrigaray R, Alkon DL (2002) MAP kinase signaling cascade dysfunction specific to Alzheimer's disease in fibroblasts. *Neurobiol Dis* **11**, 166-183.

[29] Youmans KL, Tai LM, Kanekiyo T, Stine WB Jr, Michon SC, Nwabuisi-Heath E, Manelli AM, Fu Y, Riordan S, Eimer WA, Binder L, Bu G, Yu C, Hartley DM, LaDu MJ (2012) Intraneuronal Aβ detection in 5×FAD mice by a new Aβ-specific antibody. *Mol Neurodegener* **7**, 8.

[30] Chen JQ, Heldman MR, Herrmann MA, Kedei N, Woo W, Blumberg PM, Goldsmith PK (2013) Absolute quantitation of endogenous proteins with precision and accuracy using a capillary Western system. *Anal Biochem* **442**, 97-103.

[31] Hoshi M, Sato M, Matsumoto S, Noguchi A, Yasutake K, Yoshida N, Sato K (2003) Spherical aggregates of β-amyloid (amylospheroid) show high neurotoxicity and activate Tau protein kinase I/glycogen synthase kinase-3β. *Proc Natl Acad Sci U S A* **100**, 6370-6375.

[32] Noguchi A, Matsumura S, Dezawa M, Tada M, Yanazawa M, Ito A, Akioka M, Kikuchi S, Sato M, Ideno S, Noda M, Fukunari A, Muramatsu S, Itokazu Y, Sato K, Takahashi H,

Teplow DB, Nabeshima Y, Kakita A, Imahori K, Hoshi M (2009) Isolation and characterization of patient-derived, toxic, high mass amyloid β-protein (Aβ) assembly from Alzheimer disease brains. *J Biol Chem* **284**, 32895-32905.

[33] Gross GG, Junge JA, Mora RJ (2013) Recombinant probes for visualizing endogenous synaptic proteins in living neurons. *Neuron* **78**, 971-985.

[34] Briggs F, Mangun GR, Usrey WM (2013) Attention enhances synaptic efficacy and the signal-to-noise ratio in neural circuits. *Nature* **499**, 476-480.

[35] Battaini F, Pascale A, Paoletti R, Govoni S (1997) The role of anchoring protein RACK1 in PKC activation in the ageing rat brain. *Trends Neurosci* **20**, 410-415.

[36] Masliah E, Cole G, Shimohama S, Hansen L, DeTeresa R, Terry RD, Saitoh T (1990) Differential involvement of protein kinase C isozymes in Alzheimer's disease. *J Neurosci* **10**, 2113-2124.

[37] Shimohama S, Narita M, Matsushima H, Kimura J, Kameyama M, Hagiwara M, Hidaka H, Taniguchi T (1993) Assessment of protein kinase C isozymes by two-site enzyme immunoassay in human brains and changes in Alzheimer's disease. *Neurology* **43**, 1407-1413.

[38] Favit A, Grimaldi M, Nelson TJ, Alkon DL (1998) Alzheimer's-specific effects of soluble beta-amyloid on protein kinase C-alpha and -gamma degradation in human fibroblasts. *Proc Natl Acad Sci U S A* **95**, 5562-5567.